한국측량학회지, 제 29권 제 2호, 2011. 4 : pp. 157~164

RPC-based epipolar image resampling of Kompsat-2 across-track stereos

RPC를 기반으로 한 아리랑 2호 에피폴라 영상제작

Oh, Jaehong[1] · Lee, Hyoseong[2]
오재홍 · 이효성

Abstract

As high-resolution satellite images have enabled large scale topographic mapping and monitoring on global scale with short revisit time, agile sensor orientation, and large swath width, many countries make effort to secure the satellite image information. In Korea, KOMPSAT-2 (KOrea Multi-Purpose SATellite-2) was launched in July 28 2006 with high specification. These satellites have stereo image acquisition capability for 3D mapping and monitoring. To efficiently handle stereo images such as stereo display and monitoring, the accurate epipolar image generation process is prerequisite. However, the process was highly limited due to complexity in epipolar geometry of pushbroom sensor. Recently, the piecewise approach to generate epipolar images using RPC was developed and tested for in-track IKONOS stereo images. In this paper, the piecewise approach was tested for KOMPSAT-2 across-track stereo images to see how accurately KOMPSAT-2 epipolar images can be generated for 3D geospatial applications. In the experiment, two across-track stereo sets from three KOMPSAT-2 images of different dates were tested using RPC as the sensor model. The test results showed that one-pixel level of y-parallax was achieved for manually measured tie points.

Keywords : Kompsat-2, Epipolar Resampling, RPC, Stereo

1. Introduction

As High-Resolution Satellite Imagery (HRSI) has become very important geospatial information not only for military purposes, but also for civilian applications, many countries have made efforts to secure independent operation of the high performance satellites (Stoney 2008). In Korea, the Korea Multi-Purpose Satellite-2 (KOMPSAT-2) was launched in 28 July 2006 at Plesetsk Cosmodrome in Northern Russia to collect one-meter panchromatic and four-meter multi-spectral images with a 15 km swath width from a pushbroom sensor-based multi-spectral camera (MSC) (Seo *et al.* 2008).

One important application of HRSI is 3D topographic mapping and monitoring which often requires the accurate epipolar image resampling for the stereo-display environment. Since most high resolution satellites can acquire overlapping images over the same area from either single trajectory or multiple trajectories, the stereo images can be stereo-processed for 3D ground reconstruction. Accurately determined epipolar geometry is very useful for the stereo-processing by significantly reducing computational load in stereo image matching. Also, stereo-display at the digital photogrammetry workstations enables the 3D topographic mapping and monitoring by operators, and it requires accurate epipolar image resampling.

The problem is that most HRSI employ the pushbroom sensor which epipolar properties are quite different from that of the frame camera (Gupta and Hartley 1997; Kim 2000). Therefore, conventional rigorous epipolar determination and epipolar image resampling methods cannot be applied. Accordingly, many research relied on approximate models such as 2D affine (Ono 1999; Morgan 2004; Oh *et al.* 2006).

1) PhD Candidate · Civil and Environmental Engineering and Geodetic Science · the Ohio State University (E-mail:oh.174@osu.edu)
2) Corresponding author · Associate Professor · Civil Engineering · Suncheon National University (E-mail:hslee@sunchon.ac.kr)

However, the assumptions of these simpler models cannot be satisfied for many cases. First, the assumption of nearly zero AFOV (Apparent Field of View) may not be true especially for low altitude satellites with large swath width. In addition, even if the AFOV is small, the transformation from the perspective to the parallel projection has to be applied for better accuracy before the geometric model parameters are estimated. Note that the roll angle and the focal length information are required in the step. Second, the assumption of the constant attitude will be restricted for accurate sensor modeling of rather dynamic trajectory which has to be modeled with a higher polynomial order.

Recently, the piecewise method was developed by Oh *et al.* (2010) to accurately determine epipolar geometry. The method is based on iterative projections from an image to the ground, and from the ground to the paired image. The projection can be carried out based on the rigorous physical sensor models or RPC (Rational Polynomial Coefficients) which shows little difference compared to the physical sensor model. Oh *et al.* (2010) also proposed epipolar image resampling algorithm based on the piecewise approach, and the algorithm was tested for in-track IKONOS stereo images. KOMPSAT-2 acquires stereo images in across-track, and it also requires accurate epipolar curve determination and image resampling. Therefore, this study applied the piecewise approach to KOMPSAT-2 across-track stereo images to see how accurately the epipolar image resampling can be carried out by the method.

This paper is structured as follows: in section 2, the epipolar geometry of pushbroom sensor is briefly described, and followed by introduction to the piecewise approach. In section 3, the forward and backward equations of RPC are presented for the iterative projections since RPC are used as the sensor model for KOMPSAT-2 in the study. Then, the experimental results for KOMPSAT-2 across-track stereo images are presented in section 4; the summary and conclusion follow in the end.

2. Piecewise approach to epipolar geometry of pushbroom camera

Previous studies on the epipolar geometry of pushbroom sensor showed that the epipolar curve shape is hyperbola-like and the epipolar curve pairs do not exist for the entire scene contrast to the frame camera case (Gupta and Hartley 1997; Kim 2000). These properties make it difficult to establish the epipolar geometry of the pushbroom camera for the entire scene and limits accurate epipolar image resampling. Figure 1 depicts two important properties in epipolar geometry, namely straightness and existence of epipolar line pair, for the frame camera and the pushbroom camera.

Figure 1(a) is the case of frame camera where a left image point p_1 generate a straight line on the right image and right image points q_1, q_2, q_3 along the straight line generate the identical straight line on the left image. The two corresponding straight lines on the left and the right images are called an epipolar line pair. Figure 1(b) depicts that a pushbroom sensor does not satisfy these two properties. From a left image point p_1, a curve is obtained on the right image (non-straightness), and the right image points q_1, q_2, q_3 along the curve do not produce the identical curve back on the left image (non-existence of epipolar curve pair).

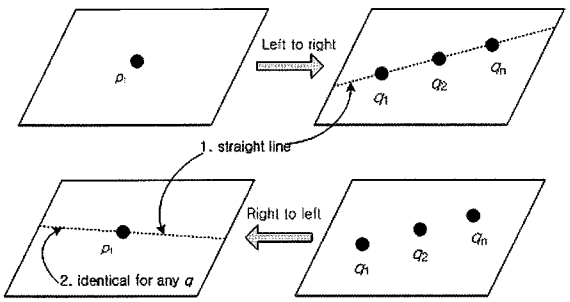

(a) Frame camera case

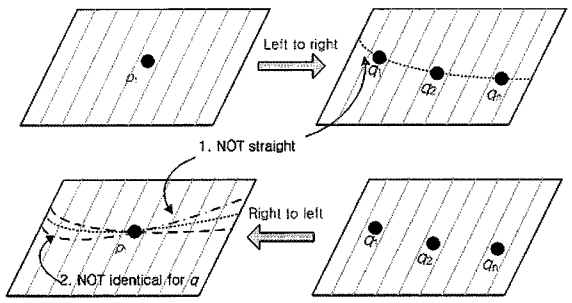

(b) Pushbroom camera case

Fig. 1. Comparison of important epipolar properties between the frame camera and the pushbroom camera.

The piecewise approach to accurately generate epipolar-resampled images was recently proposed by Oh *et al.* (2010). The authors showed the approximate existence of the epipolar curve pairs for the entire scene based on the proposed method. The epipolar image resampling algorithm consists of two main steps; the epipolar curve point generation over the entire scene, and the establishment of epipolar image transformation.

First, the epipolar curve point generation process is depicted in Figure 2. Figure 2(a) shows that the process starts from the center of the left image (p) to obtain two right image points (q_1,q_2) corresponding to the minimum and maximum ground heights. In Figure 2(b), the right image points are projected back to the left image to obtain two left image points (p', p''). The same projection is carried out iteratively as Figure 2(c). Finally, the curve point set constituting an epipolar curve can be obtained as Figure 2(d). Then along the perpendicular direction of the epipolar curve, a number of start points are established as shown in Figure 2(e), and epipolar curve points over the entire scene are obtained as Figure 2(f) by analogy. Note that the upward triangles on the left image indicate the start point locations and the downward triangles are the right image start points computed from the left image start points using the minimum ground height.

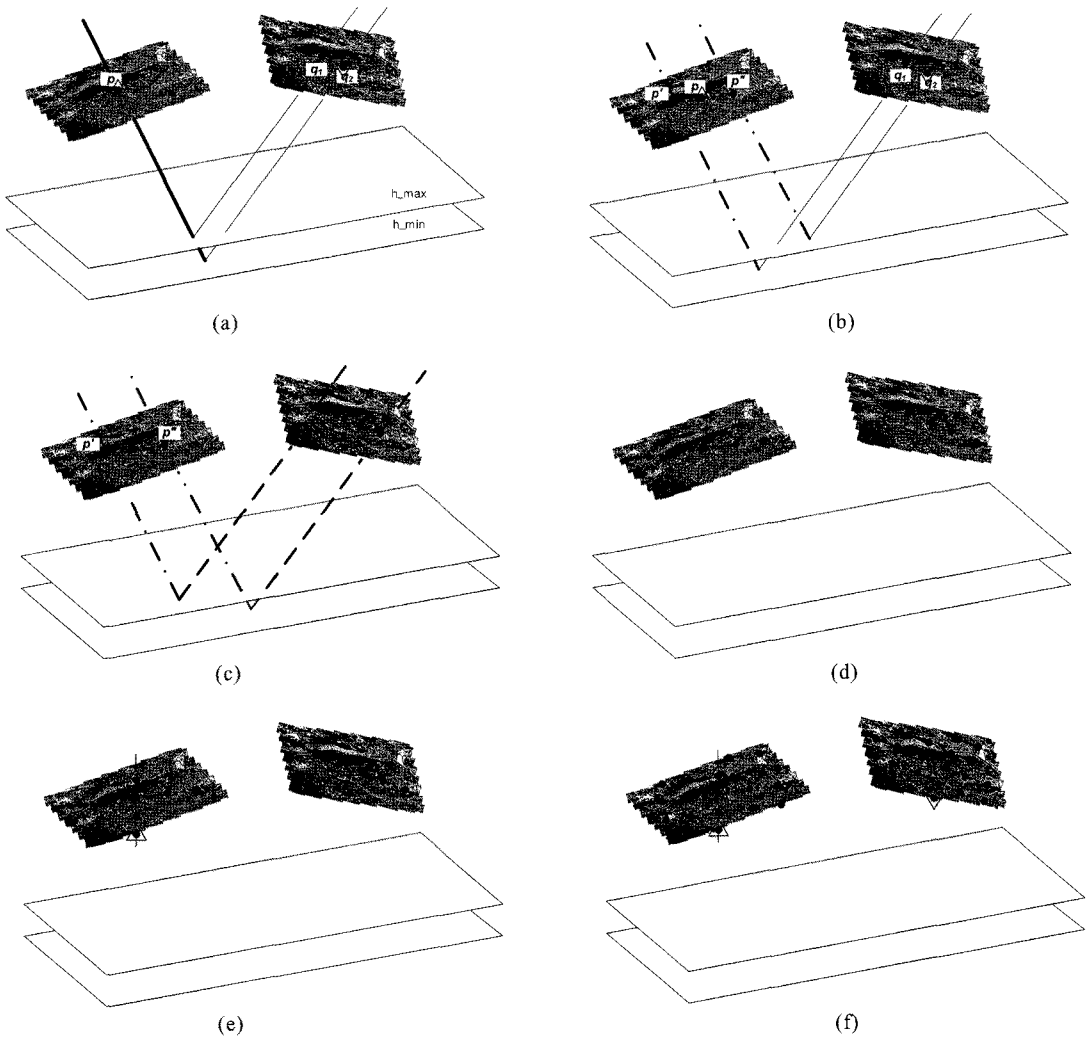

Fig. 2. The piecewise approach to generate epipolar curve points.

The piecewise approach requires iterative projections, i.e. from an image to the ground, and from the ground to the paired image. The projection equation will be presented in the following section.

The second step is the establishment of epipolar image transformation. Figure 3 shows the rearrangement of the epipolar curve points to satisfy the epipolar resampled image conditions, which is zero y-parallax and the linear relationship between the x-parallax and the ground height. First, the stereo images are aligned by lining up the start points (triangles) along the y-axis in the epipolar-resampled domain. Then the y-parallax is removed by assigning a constant row coordinate value to each epipolar curve pair in both images. The linear relationship between the x-parallax and the ground elevation can be achieved by setting the constant interval in-between the epipolar curve points. For more details, refer to (Oh *et al.* 2010).

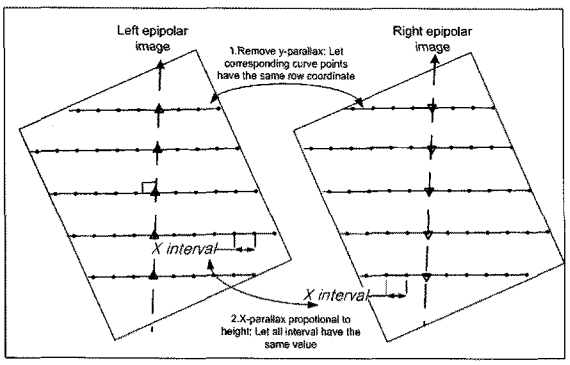

Fig. 3. Proposed epipolar resampling method from the generated epipolar curve image points (Oh *et al.* 2010).

3. RPC based projection

3.1 Ground to image projection

RPC are coefficients of RFM (Rational Function Model) which is a well known approximate sensor model. The basic RFM equation in the forward projection form, i.e., a ground coordinate to the image point coordinate, is expressed as Eq.(1)-(4) (Grodecki 2001; Dial *et a.* 2004). For the given ground coordinates the (φ,λ,h), corresponding image coordinates (l,s), can be computed. The equation is a nonlinear equation of 80 coefficients (RPC), i.e. $a_{20\times1}, b_{20\times1}, c_{20\times1}, d_{20\times1}$.

$$Y=\frac{Num_L(U,V,W)}{Den_L(U,V,W)}=\frac{a^Tu}{b^Tu},\ X=\frac{Num_s(U,V,W)}{Den_s(U,V,W)}=\frac{c^Tu}{d^Tu} \quad (1)$$

with

$$U=\frac{\varphi-\varphi_O}{\varphi_S},V=\frac{\lambda-\lambda_O}{\lambda_S},W=\frac{h-h_O}{h_S},Y=\frac{l-L_O}{L_S},X=\frac{s-S_O}{S_S} \quad (2)$$

$$\begin{aligned}u=\big[&1 \quad V \quad U \quad W \quad VU \quad VW \quad UW \quad V^2\\ &U^2 \quad W^2 \quad UVW \quad V^3 \quad VU^2 \quad VW^2 \quad V^2U\\ &U^3 \quad UW^2 \quad V^2W \quad U^2W \quad W^3\big]^T\end{aligned} \quad (3)$$

$$\begin{aligned}a=\big[a_1 \quad a_2 \quad \cdots \quad a_{20}\big]^T, b=\big[1 \quad b_2 \quad \cdots \quad b_{20}\big]^T\\ c=\big[c_1 \quad c_2 \quad \cdots \quad c_{20}\big]^T, d=\big[1 \quad d_2 \quad \cdots \quad d_{20}\big]^T\end{aligned} \quad (4)$$

where, X,Y are the normalized image space coordinates, U,V,W are the normalized object space coordinates, ϕ,λ,h are the geodetic latitude, longitude and ellipsoidal height, l,s are the image line (row) and sample (column) coordinates, $\phi_0,\lambda_0,h_0,S_0,L_0$ are the offset factors for the latitude, longitude, height, sample and line, and $\phi_S,\lambda_S,h_S,S_S,L_S$ are the scale factors for the latitude, longitude, height, sample and line

3.2 Image to ground projection (to the fixed ground height)

Given an image point, (l,s), and given height (h), the horizontal ground coordinate can be computed from RFM. The given information should be normalized first as Eq.(2). Since the RFM is not in linear form, The Taylor series expansion is applied first to obtain the linearized RFM equation. Note that the initial horizontal ground coordinate is required for the expansion, and it can be obtained from the first order terms by neglecting higher order terms in RFM as Eq.(5), which can be expressed as Eq.(6).

$$Y=\frac{a_1+a_2V^0+a_3U^0+a_4W}{b_1+b_2V^0+b_3U^0+b_4W},\ X=\frac{c_1+c_2V^0+c_3U^0+c_4W}{d_1+d_2V^0+d_3U^0+d_4W} \quad (5)$$

$$\Rightarrow\begin{bmatrix}V^0\\U^0\end{bmatrix}=\begin{bmatrix}(Yb_2-a_2) & (Yb_3-a_3)\\(Xd_2-c_2) & (Xd_3-c_3)\end{bmatrix}^{-1}\begin{bmatrix}a_1+(a_4-Yb_4)W-Yb_1\\c_1+(c_4-Xd_4)W-Xd_1\end{bmatrix} \quad (6)$$

Now that the initial normalized horizontal ground coordinates (V^0, U^0) are computed, the linearization of RFM is obtained with respect to the normalized horizontal ground coordinate (V, U) as Eq. (7).

$$Y = Y^0 + \left.\frac{\partial Y}{\partial V}\right|^0 dV + \left.\frac{\partial Y}{\partial U}\right|^0 dU,\ X = X^0 + \left.\frac{\partial X}{\partial V}\right|^0 dV + \left.\frac{\partial X}{\partial U}\right|^0 dU \quad (7)$$

where

$$Y^0 = \frac{a^T u^0}{b^T u^0},\ X^0 = \frac{c^T u^0}{d^T u^0} \quad (8)$$

$$\boldsymbol{u}^0 = \left[1\ \ V^0\ \ U^0\ \ W\ \ V^0U^0\ \ V^0W\ \ U^0W\ \ (V^0)^2\ \ (U^0)^2\ \ W^2\ \ U^0V^0W\ \ (V^0)^3\ \ V^0(U^0)^2\ \ V^0W^2\ \ (V^0)^2U^0\ \ (U^0)^3\ \ U^0W^2\ \ (V^0)^2W\ \ (U^0)^2W\ \ W^3\right]^T \quad (9)$$

The coefficients in Eq.(7) are obtained by chain rules as Eqs.(10), (11), and (12).

$$\frac{\partial Y}{\partial V} = \frac{\partial Y}{\partial u^T}\frac{\partial u}{\partial V},\ \frac{\partial Y}{\partial U} = \frac{\partial Y}{\partial u^T}\frac{\partial u}{\partial U},\ \frac{\partial X}{\partial V} = \frac{\partial X}{\partial u^T}\frac{\partial u}{\partial V},\ \frac{\partial X}{\partial U} = \frac{\partial X}{\partial u^T}\frac{\partial u}{\partial U} \quad (10)$$

with

$$\frac{\partial Y}{\partial u^T} = \frac{\frac{\partial (a^T u)}{\partial u^T}(b^T u) - (a^T u)\frac{\partial (b^T u)}{\partial u^T}}{(b^T u)^2} = \frac{(b^T u)a^T - (a^T u)b^T}{(b^T u)^2},\ \frac{\partial X}{\partial u^T} = \frac{(d^T u)c^T - (c^T u)d^T}{(d^T u)^2} \quad (11)$$

$$\frac{\partial u}{\partial U} = \left[0\ 0\ 1\ 0\ V\ 0\ W\ 0\ 2U\ 0\ VW\ 0\ 2VU\ 0\ V^2\ 3U^2\ W^2\ 0\ 2UW\ 0\right]^T$$
$$\frac{\partial u}{\partial V} = \left[0\ 1\ 0\ 0\ U\ W\ 0\ 2V\ 0\ 0\ UW\ 3V^2\ U^2\ W^2\ 2VU\ 0\ 0\ 2VW\ 0\ 0\right]^T \quad (12)$$
$$\frac{\partial u}{\partial W} = \left[0\ 0\ 0\ 1\ 0\ V\ U\ 0\ 0\ 2W\ UV\ 0\ 0\ 2VW\ 0\ 0\ 2UW\ V^2\ U^2\ 3W^2\right]^T$$

The incremental coordinates can be solved by Eq.(13) and the normalized horizontal ground coordinate is updated as Eq.(14). Through the iterative estimation until the increment is ignorable, the normalized horizontal ground coordinate can be computed. Finally, by unnormalizing them using Eq.(2), the horizontal ground coordinates, (φ, λ), are obtained.

$$\begin{bmatrix} dV \\ dU \end{bmatrix} = \begin{bmatrix} \left.\frac{\partial Y}{\partial V}\right|_{V=V^0} & \left.\frac{\partial Y}{\partial U}\right|_{U=U^0} \\ \left.\frac{\partial X}{\partial V}\right|_{V=V^0} & \left.\frac{\partial X}{\partial U}\right|_{U=U^0} \end{bmatrix}^{-1} \begin{bmatrix} Y - Y^0 \\ X - X^0 \end{bmatrix} \quad (13)$$

$$\begin{bmatrix} V \\ U \end{bmatrix} = \begin{bmatrix} V^0 \\ U^0 \end{bmatrix} + \begin{bmatrix} dV \\ dU \end{bmatrix} \quad (14)$$

4. Experiment

4.1 Data specification

Three KOMPSAT-2 images were tested for the piecewise method. Table 1 presents the specification of each tested image. The target area is Daegu, Korea which location is about 35.89°N and 128.49°E, and the terrain elevation range is about 400 meters. Note that each image was acquired in different date and trajectory, i.e. across-track. From the bundle-adjusted aerial images, total 39 ground control points and 38 check points were acquired over the entire area for accuracy check purpose. Figure 4 depicts the distribution of ground points over the data set.

Table 1. Tested KOMPSAT-2 data specification

Data	Level	Site	Date	Incidence / Azimuth	Image size	Spectral
K1	1R	Daegu, Korea	2009-01-03	6.2° / 249.1°	15,500 × 15,000	PAN
K2	1R	Daegu, Korea	2009-12-31	14.1° /256.1°	15,500 × 15,000	PAN
K3	1R	Daegu, Korea	2010-02-07	5.8° /91.7°	15,500 × 15,000	PAN

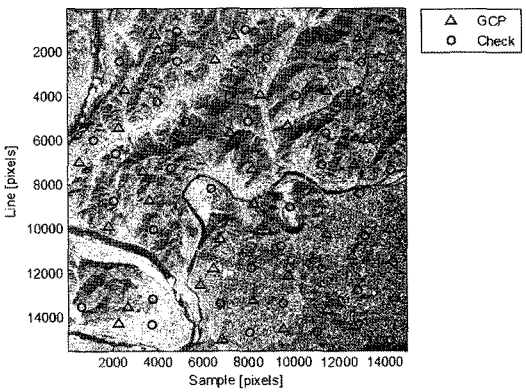

Fig. 4. Ground control points and check points distribution on K1 image.

Table 2 shows that two stereo set are tested, named S1 for the pair K1-K3, and S2 for the pair K2-K3. The pair K1-K2 was not tested because the pair has little convergence angle. Note that S1 and S2 also do not have decent convergence angle (computed from the provided incidence and azimuth) showing less than 20 degrees.

Table 2. Stereo combination

Stereo	Data	Convergence angle
S1	K1-K3	11.77°
S2	K2-K3	19.75°

4.2 RPC correction

Before the epipolar image generation, the RPC correction was attempted using the ground control points based on the well-known affine model (Dial and Grodecki 2002; Fraser and Hanley 2005). Table 3 presents the positional accuracy of corrected RPC for the check points. RMSE for K2 and K3 was around one-pixel level while K1 showed slightly low accuracy along the line direction.

Table 3. Positional accuracy of RPC correction

RPC Correction		RMSE [sample/line] [pixel]
Affine	K1	1.00 / 1.46
	K2	0.99 / 0.99
	K3	0.86 / 0.87

4.3 Epipolar curve points generation

The piecewise approach was applied to the stereo set S1 and S2. The height range (0m, 500m) was used for the iterative projection, and the interval in-between epipolar curve was established to 1000 pixels. Figure 5 depicts the generated epipolar curve points with starting points (triangles) for S1. Note that the curves are not straight yet, even though it looks like straight on the graph due to the display scale.

4.4 Epipolar Images generation

The generated epipolar curve points in Figure 5 were rearranged to satisfy the epipolar image conditions, and the result is presented in Figure 6. The epipolar curve is now straightened along the column direction, i.e. the y coordinates for each epipolar line points are same. Note that the distance in between curve points are now same.

Based on the correspondence between the epipolar curve points and rearranged points, the second order polynomial image resampling transformation was applied. Table 4 pre-

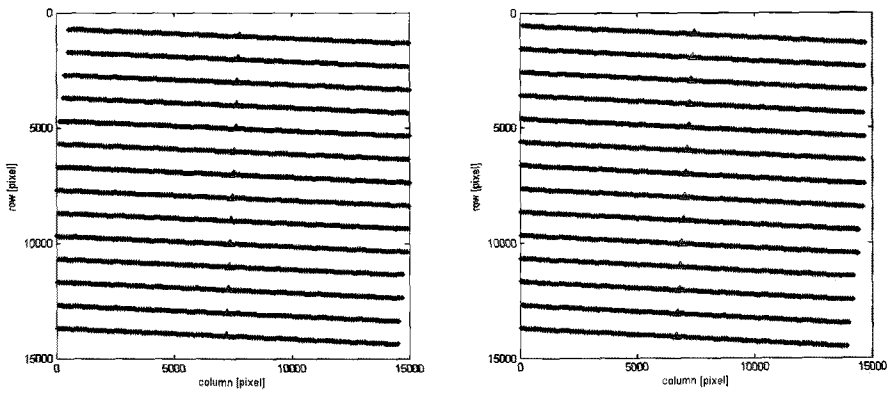

Fig. 5. Generated epipolar curve points for S1 (left: K1, right: K3)

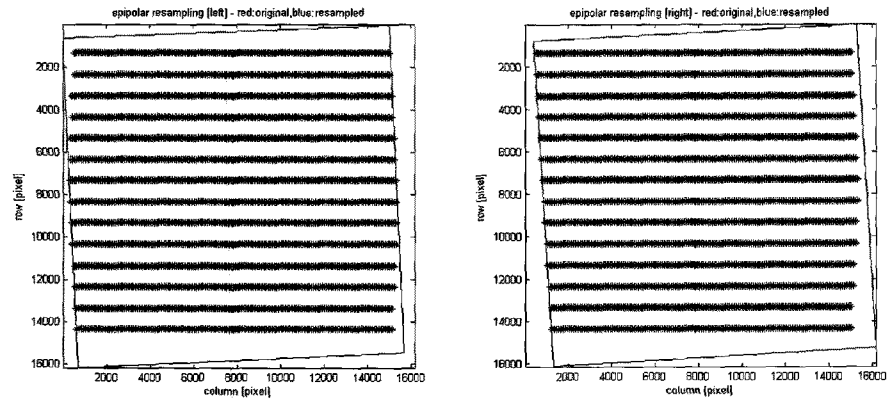

Fig. 6. Rearranged epipolar curve points for S1 (left: resampled K1, right: resampled K3)

sents the epipolar image resampling result and Figure 7 is the epipolar-resampled images in colored anaglyph. The ground accuracy was checked for all 39 ground control points and 38 check points shown in Table 4. S1 and S2 showed one-pixel level of y-parallax and one-meter level of horizontal ground restitution accuracy while the vertical ground accuracy was two or three meters level. Accounting for the low convergence angle, the accuracy seems decent. Note that achievable y-parallax is mostly dependent on the accuracy of sensor models used and the image measurement accuracy of check points. In other words, near zero y-parallax can be secured if the sensor model is perfect and there is no image measurement error (Oh *et al.* 2010).

Table 4. Epipolar image resampling result

Stereo	y-parallax RMSE [pixels]	Ground RMSE [meters] [X/Y/Z]
S1 (K1-K3)	1.01	1.08 / 1.11 / 3.26
S2 (K2-K3)	0.79	1.14 / 0.99 / 2.23

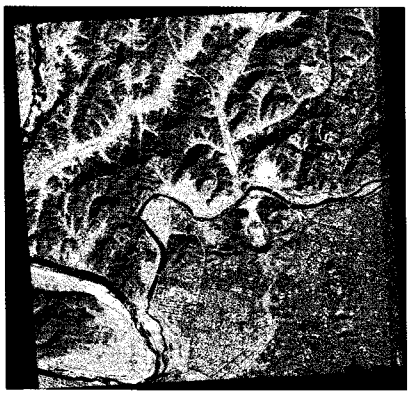

(a) S1 (K1-K3)

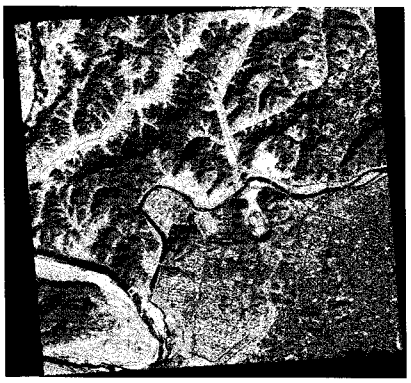

(b) S2 (K2-K3)

Fig. 7. Generated epipolar images (anaglyph)

5. Conclusion

Stereo high resolution satellite images are very useful information for 3D topographic mapping and monitoring. Among the stereo image preprocessing, accurate epipolar geometry determination and epipolar image resampling would be the most important step. However, the process was highly limited due to complexity in epipolar geometry of pushbroom sensor. But recently, a new piecewise method was developed and tested for IKONOS images to efficiently handle the epipolar geometry for accurate epipolar image resampling. KOMPSAT-2 also can acquire stereo images in across-track, and it requires the accurate epipolar image resampling to be used for 3D geospatial applications. Therefore, this study tested the recently developed piecewise method to KOMPSAT-2 across-track stereo images to see how accurately epipolar images can be generated.

Two stereo sets were selected and tested from three overlapping KOMPSAT-2 images of different dates, i.e., acquired in across-track. First, the accuracy of KOMPSAT-2 RPC was improved up to near one-pixel level using well-distributed ground controls. Second, the newly developed piecewise method was applied to the two stereo sets. Then, accurate epipolar image generation was carried out. The test results clearly showed that the epipolar image generation was successful showing one-pixel level of y-parallax, which was introduced by RPC accuracy and observation accuracy of tie points. Even though the stereo sets do not have decent convergence angle, the ground restitution accuracy was one meter level in horizontal and two or three meters in vertical.

Acknowledgement

The authors would like to thank KARI (Korea Aerospace Research Institute) for providing the KOMPSAT-2 data.

References

Dial, G. and Grodecki J. (2002), Block adjustment with rational polynomial camera models, *Proceedings of the ACSM-ASPRS 2002 Annual Conference*, ASPRS, Washington DC, unpaginated CD-ROM.

Fraser, C.S. and Hanley, H.B. (2005), Bias-compensated RPC for sensor orientation of high-resolution satellite imagery, *Photogrammetric Engineering & Remote Sensing*, ASPRS, Vol. 71, No. 8, pp. 909-915.

Fraser, C.S. and Ravanbakhsh, M. (2009), Georeferencing accuracy of GeoEye-1 imagery, *Photogrammetric Engineering & Remote Sensing*, ASPRS, Vol. 75, No. 6, pp. 634-638.

Grodecki, J. (2001), IKONOS stereo feature extraction - RPC approach, *Proceedings of ASPRS 2001 Annual Convention*, ASPRS, St. Louis, Missouri, unpaginated CD-ROM.

Grodecki, J., Dial, G. and Lutes, J. (2004), Mathematical model for 3D feature extraction from multiple satellite images described by RPC. *Proceedings of the ASPRS 2004 Annual Conference*, ASPRS, Denver, Colorado, unpaginated CD-ROM.

Gupta, R. and Hartley, R. (1997), Linear Pushbroom Cameras, IEEE *Transactions on pattern analysis and machine intelligence*, IEEE TPAMI, Vol. 19, No. 9, pp. 963-975.

Kim, T. (2000), A Study on the epipolarity of linear pushbroom images, *Photogrammetric Engineering & Remote Sensing*, ASPRS, Vol. 66, No. 8, pp. 961-966.

Morgan, M. (2004), Epipolar resampling of linear array scanner scene, PhD dissertation, University of Calgary, Calgary, Alberta.

Oh, J. H., Shin, S.W. and Kim, K. (2006), Direct Epipolar Image generation From IKONOS Stereo Imagery Based on RPC and Parallel Projection Model, *Korean Journal of Remote Sensing*, KSRS, Vol. 22, No. 5, pp. 451-456.

Oh, J. H., Lee, W.H., Toth, C.K., Grejner-Brzezinska, D.A. and Lee, C.N. (2010), A Piecewise Approach to Epipolar Resampling of Pushbroom Satellite Images Based on RPC, *Photogrammetric Engineering & Remote Sensing*, ASPRS, Vol. 76, No. 12, pp. 1353-1363.

Ono, T. (1999), Epipolar Resampling of High resolution satellite imagery, *International Archives of Photogrammetry and Remote Sensing*, the Joint Workshop of ISPRS WG I/1, I/3 and IV/4 on Sensors and Mapping from Space, ISPRS, Hannover, unpaginated CD-ROM.

Seo, D.C., Yang, J. Y., Lee, D. H., Song, J. H. and Lim, H. S. (2008), Kompsat-2 Direct Sensor Modeling and Geometric Calibration/Validation, *The International Archives of the Photogrammetry, Remote Sensing and Spatial Information Sciences*. ISPRS, Beijing, Vol. XXXVII. Part B1.

Stoney, W. E. (2008), ASPRS Guide to Land Imaging Satellites, http://www.asprs.org/news/satellites/satellites.html.

(접수일 2011. 03. 31, 심사일 2011. 04. 12, 심사완료일 2011. 04. 12)